THE JOURNAL OF BIOLOGICAL CHEMISTRY VOL. 289, NO. 43, pp. 29994–30004, October 24, 2014

Loss of TRB3 Alters Dynamics of MLK3-JNK Signaling and Inhibits Cytokine-activated Pancreatic Beta Cell Death*[S]

Received for publication, April 23, 2014, and in revised form, August 11, 2014 Published, JBC Papers in Press, September 9, 2014, DOI 10.1074/jbc.M114.575613

Rohan K. Humphrey, Anamika Ray, Sumati Gonuguntla, Ergeng Hao, and Ulupi S. Jhala[1]

From the Pediatric Diabetes Research Center, University of California, San Diego School of Medicine, La Jolla, California 92037

Background: MLK3 induces TRB3 to inhibit AKT and compromise beta cell survival.
Results: AKT regulates novel phosphorylation, ubiquitination, and degradation of MLK3, explaining why TRB3$^{-/-}$ islets display attenuated MLK3/JNK activation and beta cell death.
Conclusion: TRB3 functionally cooperates with the JNK module to fine-tune inflammatory signaling in beta cells.
Significance: Even modest modulation of signaling dynamics can alter inflammatory outcomes.

Disabling cellular defense mechanisms is essential for induction of apoptosis. We have previously shown that cytokine-mediated activation of the MAP3K MLK3 stabilizes TRB3 protein levels to inhibit AKT and compromise beta cell survival. Here, we show that genetic deletion of TRB3 results in basal activation of AKT, preserves mitochondrial integrity, and confers resistance against cytokine-induced pancreatic beta cell death. Mechanistically, we find that TRB3 stabilizes MLK3, most likely by suppressing AKT-directed phosphorylation, ubiquitination, and proteasomal degradation of MLK3. Accordingly, TRB3$^{-/-}$ islets show a decrease in both the amplitude and duration of cytokine-stimulated MLK3 induction and JNK activation. It is well known that JNK signaling is facilitated by a feed forward loop of sequential kinase phosphorylation and is reinforced by a mutual stabilization of the module components. The failure of TRB3$^{-/-}$ islets to mount an optimal JNK activation response, coupled with the ability of TRB3 to engage and maintain steady state levels of MLK3, recasts TRB3 as an integral functional component of the JNK module in pancreatic beta cells.

Cytokine-induced beta cell failure and death are crucial events that lead to type 1 as well as type 2 diabetes (1). Cytokines rapidly activate the stress kinase SAPK/JNK, and other proinflammatory kinases, setting in motion a series of events that unfold over several hours and cumulatively lead to dysfunction and demise of the beta cell (1–3). JNK activation has been clearly linked to mitochondrial stress and damage in multiple cell types, including the pancreatic beta cell (4–6). We have reported that cytokine-induced MLK3-JNK pathway is instrumental in compromising mitochondrial integrity early in the apoptotic process, effectively reducing cellular defenses and increasing the potency of subsequent inflammatory events (6).

Signaling via the JNK module results from the sequential activation of a MAP3K, MAP2K, and JNK, complexed via a scaffold protein (7, 8). Cytokine binding to cognate TNF and IL-1/TLR receptors triggers activation of the TRAF[2] family of atypical ubiquitin ligases and promotes Lys-63-linked ubiquitination and autophosphorylation of MAP3Ks (9–11), including MLK3 (12–14). A series of reports have provided biological proof that cytokines favor JNK activation via the specific MLK3-MKK7-JNK-JIP1 signaling module (15–17). Furthermore, robust JNK signaling is facilitated by a self-amplifying, feed-forward loop of sequential kinase phosphorylation and is reinforced by mutual stabilization of the signaling module components (18).

We have previously shown that MLK3 activation and protein levels are both induced by IL-1β stimulation of mouse and human islets. Along with MLK3, IL-1β also stimulates tandem induction of TRB3 protein expression in pancreatic islets (6). Furthermore, in the beta cell, MLK3 engagement stabilizes TRB3 protein levels to suppress AKT survival kinase and facilitate downstream proinflammatory effects of IL-1β (6). Here, we report that AKT directly phosphorylates MLK3 at a novel site (Thr-477) located adjacent to the leucine zipper domain, triggering Lys-48-linked ubiquitination and proteasomal degradation of MLK3. Our results also show that the ubiquitin acceptor site instrumental for triggering degradation of MLK3, coincides with the acceptor site for TRAF6-dependent Lys-63-linked ubiquitination and activation of MLK3. This site-specific convergence of functionally divergent ubiquitination events, shows that ubiquitination of MLK3 (Lys-48 *versus* Lys-63) plays a crucial role in driving cytokine-mediated beta cell death.

Consistent with the above mechanism, TRB3 null islets displayed higher levels of active AKT and attenuated cytokine-stimulated MLK3 induction and JNK activation. More importantly, TRB3$^{-/-}$ islets also displayed resistance to cytokine-mediated beta cell death. We conclude that cytokines require a threshold of proinflammatory signal activation for inducing beta cell death and that TRB3 is required for optimal kinetics of MLK3-JNK activation to enable cell death. Taken together, these data suggest that factors responsible for fine-tuning the dynamics of cytokine signaling can be exploited for therapeutic intervention.

* This work was supported by National Institutes of Health Grant R01DK080147, Juvenile Diabetes Research Foundation Research Grant 40-2009-706, and a Hillblom Foundation Network Grant.
[S] This article contains supplemental Figs. 1 and 2.
[1] To whom correspondence should be addressed: Pediatric Diabetes Research Center, 3525 John Hopkins Court, San Diego, CA 92121. Tel.: 858-822-2072; E-mail: ujhala@ucsd.edu.

[2] The abbreviation used is: TRAF, TNF receptor-associated factor; KD, kinase-dead.

EXPERIMENTAL PROCEDURES

TRB3 Knock-out Mice—The mutant mouse strain was obtained from the European Mouse Mutant Archive (EMMA ID EM:02346), Helmholtz Zentrum Muenchen, Germany. Briefly, the strain was generated by retroviral insertion of a gene trap vector encoding a premature stop codon prior to the first coding exon and was originally developed by Lexicon Genetics, Inc., under the Wellcome Trust Knock-out Mouse Resource. Mice were housed in a 12-h light/12-h dark cycle at controlled temperature (25 °C ± 1 °C). Genotyping was performed by PCR of genomic DNA according to above referenced protocols. In experimental procedures, we compared homozygous TRB3 knock-out mice with wild-type littermates (control mice). All experimental procedures were performed according to University of California San Diego Institutional Animal Care and Use Committee policies.

Reagents—Antibodies used for Western blotting include anti-MLK3, pMLK3, JNK, pJNK, GST, AKT, pAKT, Myc, FLAG, anti-AKT-substrate, β-tubulin (Cell Signaling, Beverly, MA), and anti-TRB3 (Dr. Marc Montminy, Salk Institute, CA). For immunofluorescence, mouse anti-BAX clone 6A7 (BD Biosciences), sheep anti-insulin (Binding Site), rabbit anti-GST (Cell Signaling), and *In Situ* Cell Death Detection Kit (fluorescein) from Roche Diagnostics were purchased from commercial sources. Glutathione-Sepharose beads (Amersham Biosciences) were used for pulldown experiments. Fluorescence and Western blotting employed fluorescent or HRP-conjugated secondary antibodies (Jackson ImmunoResearch Laboratories, West Grove, PA), the latter was detected using Supersignal chemiluminescence reagents (Pierce Biotechnology, Inc.). Other reagents include CEP11004 (Cephalon, Inc., Frazer, PA), AKT inhibitor VII, cycloheximide, thapsigargin (EMD Biosciences, San Diego, CA), IL-1β, TNF-α, IFN-γ (Peprotech, Rocky Hill, NJ), and insulin (Humulin Eli-Lily).

Plasmids and Constructs—PEBG-MLK3-WT and kinase-dead (KD), PEBG-JNK, HA-TRB3, HA-AKT, and FLAG-β-tubulin, and Myc-ubiquitin WT constructs have been described elsewhere (6). All MLK3 and Myc-ubiquitin K48R point mutants were generated by site-directed mutagenesis using the QuikChange mutagenesis protocol (Stratagene, Inc.).

Cell Culture and Transfection—Min6 cells (passages 15–18 only) were grown in DMEM containing 25 mM glucose supplemented with 4% heat-inactivated FBS and 50 μM β-mercaptoethanol. HEPG2 cells were grown in a 1:1 mix of DMEM and F12K and 5% heat-inactivated FBS. Transfections were carried out using Lipofectamine 2000 (Invitrogen) as per the manufacturer's instructions and were treated as described 48 h post transfection. For the TUNEL assay, Min6 cells were treated for 8 h with a mixture of 10 nM TNF-α, 40 ng/ml IFN-γ, and 20 ng/ml IL-1β, ~20 h post-transfection.

GST Pulldown Assay—Mammalian expression vectors encoding GST fusion proteins were expressed in Min6 or HepG2 cells followed by GST pulldowns with glutathione Sepharose (Amersham Biosciences) as described (6).

MLK3 Ubiquitination—Experiments were performed as described (14). Briefly, 40–48 h post-transfection, cells were treated with insulin as described, harvested in 1% SDS, 50 mM Tris, pH 8.0, 1 mM EDTA containing phosphatase inhibitors, and 10 mM *N*-ethylmaleimide deubiquitinase inhibitor. Lysates were boiled, cooled on ice, sonicated, and precleared with Sepharose beads, and the supernatants diluted 5-fold with dilution buffer (150 mM NaCl, 20 mM Tris, pH 8.0, 1 mM EDTA) with a full complement of phosphatase and protease inhibitors and deubiquitinase inhibitor (*N*-ethylmaleimide), used for GST pulldowns, resolved by SDS-PAGE, and probed using anti-Myc antibodies. Blots were stripped and probed using anti-GST antibodies for GST-MLK3 input.

Cycloheximide Chase, Western Blotting, and Insulin Stimulation—Experiments were performed as described (47).

AKT-mediated in Vitro Phosphorylation of MLK3—GST-MLK3-WT, T477A, S674A, and double mutant (TS-AA), were expressed in HepG2 cells, and the cells were pretreated with AKT inhibitor for 4 h and CEP11004 for 1 h. GST-MLK3-WT and mutant proteins were isolated using GST pulldown, and expression levels were assessed using Coomassie staining, and anti-GST Western blots. Equal amounts of GST-bound MLK3 proteins (WT and mutants) were incubated with recombinant AKT1 (EMD Biosciences, San Diego, CA) for 40 min at 30 °C in kinase assay buffer (200 μM ATP, 20 mM Tris-HCl, pH 7.5, 10 mM $MgCl_2$, 10 mM DTT, and 100 nM CEP11004) using [γ-^{32}P]ATP. Following SDS-PAGE, phosphoproteins were detected by autoradiography.

Splenocyte and Islet Co-Culture—Co-culture was performed as described previously with some modifications (6). Briefly, wild-type spleens were crushed and passed through a 70-μm mesh. Red blood cells were lysed in 0.15 M NH_4Cl and 1.5×10^6 splenocytes per well were plated in 24-well dishes in RPMI supplemented with 10% heat-inactivated FBS. Splenocytes were stimulated with plate-bound anti-CD3 and exogenous anti-CD28 antibodies (10 μg/ml and 1 μg/ml, respectively; BD Biosciences) for 2 days. Isolated islets from WT or TRB3$^{-/-}$ mice were rested overnight and co-cultured using Transwell filters in the presence of unstimulated or stimulated splenocytes.

Immunofluorescence and TUNEL Assays—Islets were fixed in zinc-buffered formalin (Anatech, Battle Creek, MI) for 1 h and processed for routine cryomicrotomy. Min6 cells were fixed in 2% paraformaldehyde for 10 min, and both the cells and frozen sections were permeabilized using 0.1% Triton X-100, and the TUNEL assay was carried out according to the manufacturer's instructions (Roche Diagnostics). Primary antibodies were visualized with species-specific secondary antibodies conjugated to fluorescent probes.

Microscopy and Image Acquisition—Fluorescent images were acquired on a Zeiss 710 confocal microscope. All images were assembled in Photoshop CS6, (Adobe Systems, Inc., San Jose, CA) and NIH ImageJ software. Quantification was performed on 10 randomly selected fields of view using the 40 or 60× objective from three separate experiments. Total cell counts were obtained using DAPI (1 μg/ml) nuclear counterstaining.

Statistics—Differences between means were examined using analysis of variance followed by a Bonferroni post hoc comparison. In all cases, p values ≤ 0.05 were considered significant. Analysis was performed using GraphPad Prism software.

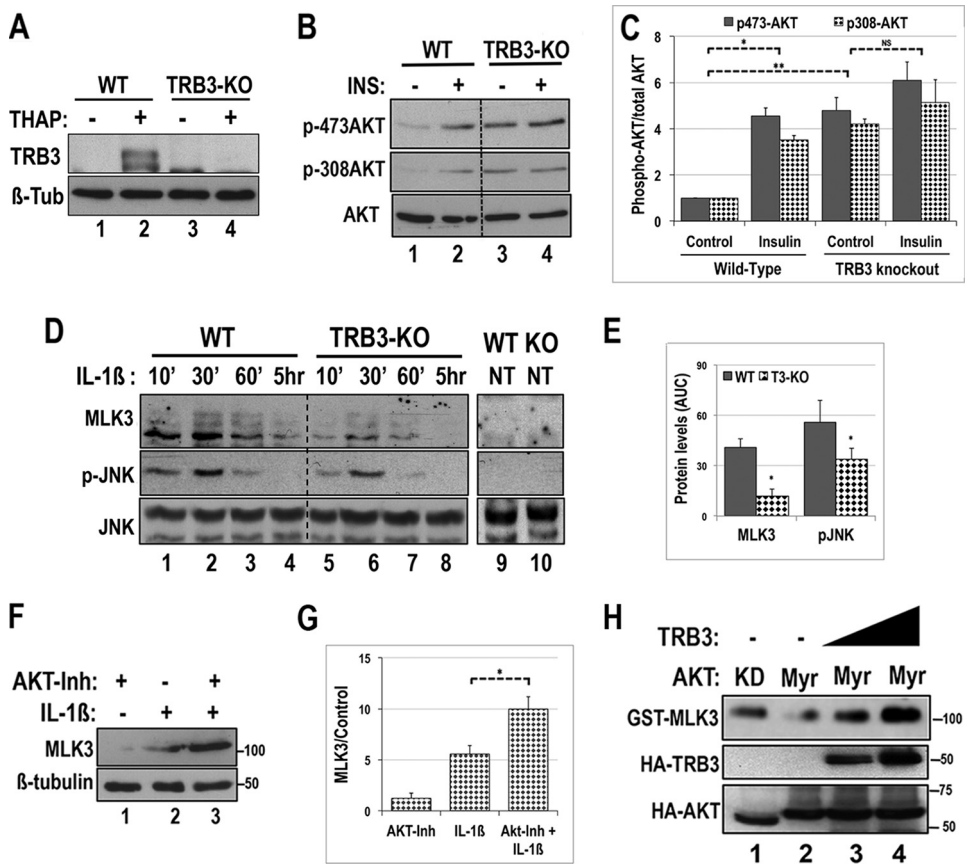

FIGURE 1. **TRB3 null islets display basal AKT activity and attenuated activation of MLK3 and JNK.** *A*, wild-type (*lanes 1* and *2*) and TRB3 knock-out (TRB3-KO, *lanes 3* and *4*) islets were treated with 1 μM thapsigargin (*THAP*, *lanes 2* and *4*) for 16 h, and total cell lysates were assessed for TRB3 protein expression using SDS-PAGE followed by Western blotting using anti-TRB3 antibodies. β-Tubulin (β-*Tub*) was used as a loading control. *B*, WT (*lanes 1* and *2*) and TRB3-KO (*lanes 3* and *4*) islets were treated with insulin (*INS*; *lanes 2* and *4*) for 10 min, and total cell lysates were analyzed by Western blotting using AKT antibodies specific for phospho-Ser4–73 and Thr-308. Total AKT levels are shown. *C*, densitometric analysis of AKT phosphorylation in WT and TRB3-KO islets represent means ± S.E. of three separate experiments. * and **, $p < 0.05$ *versus* untreated WT control. *NS*, not significant. *D*, WT (*lanes 1–4*) and TRB3-KO (*lanes 5–8*) islets were treated with 20 ng/ml of IL-1β for the indicated times, and lysates (60 μg protein) were subjected to Western blotting using anti-MLK3 and phospho-JNK antibodies. Total JNK protein levels are shown. Expression under unstimulated conditions (*NT*) in WT and TRB3-KO islets is shown (*lanes 9* and *10*). *E*, densitometric analyses of time-dependent MLK3 induction and JNK activation from WT and TRB3-KO islets were graphed, and total kinase induction/activity over time was assessed by calculating area under the curve (*AUC*). Average values from three independent experiments are presented as a bar graph. *, $p < 0.05$ *versus* WT islets. *F*, Min6 cells incubated for 30 min (*30′*) in the presence (*lanes 1* and *3*) or absence (*lane 2*) of a synthetic inhibitor of AKT enzymatic activity were treated with IL-1β for 20 min (*lanes 2* and *3*), and total cell lysates were subjected to SDS-PAGE followed by Western blotting for endogenous MLK3 expression. β-Tubulin served as a loading control. *G*, densitometric quantitation of MLK3 protein levels normalized to β-tubulin shown as the mean ± S.E. from three separate experiments. *, $p < 0.05$ *versus* IL-1β treatment in the absence of AKT inhibitor (*inh*). *H*, GST-MLK3 was expressed in HepG2 cells with KD (*lane 1*) or myristoylated (*Myr*) (*lanes 2–4*) AKT in the absence (*lanes 1* and *2*) or presence of increasing amounts of HA-tagged pseudokinase protein TRB3 (*lanes 3* and *4*). Cellular extracts were used for GST pulldowns and probed for total MLK3 levels using anti-GST antibodies. Lysate inputs were used for Western blotting of HA-TRB3 and HA-AKT.

RESULTS

TRB3 Is Required for Optimal MLK3-JNK Activation—We have previously reported that the MAP3K MLK3 and the pseudokinase TRB3 are both induced by IL-1β and function in concert to diminish survival mechanisms in cytokine-treated beta cells. Pseudokinases, although lacking in catalytic activity, function as allosteric modulators of other kinases, most likely in a context-dependent manner (19). The absence of a consistent and reliable readout for TRB3 action necessitates a more empirical exploration of TRB3 function. Published data suggest that TRB3$^{-/-}$ mice display normal glucose homeostasis on a chow-fed regimen as assessed by glucose and insulin tolerance tests (20). To better understand the role of TRB3 in pancreatic beta cells, we obtained whole body TRB3 knock-out mice that were generated at source as described. The mice bred in normal Mendelian ratios, and based on growth, weight, and glucose tolerance tests, TRB3$^{-/-}$ mice were indistinguishable from WT littermates, and we observed no discernable effect on pancreatic beta cell mass and size (data not shown). We verified TRB3 ablation using isolated islets pooled from multiple TRB3$^{-/-}$ or WT mice. As seen in Fig. 1*A*, thapsigargin strongly induced TRB3 protein levels in WT islets, and no signal was observed in TRB3$^{-/-}$ islets (compare *lanes 2* and *4*). Notably, TRB3 protein was not detected in the absence of stress in WT islets. Similar data were observed for TRB3 mRNA levels (supplemental Fig. S1).

Several studies have shown that TRB3 functions as a potent inhibitor of AKT kinase in multiple contexts (21–24). Generally, pancreatic islets display high basal levels of AKT kinase activation, most likely a result of glucose-stimulated insulin secretion and autocrine insulin signaling (25, 26). We observed no difference in the levels of total or phosphorylated AKT protein under normal culture conditions (data not shown) in islets of WT *versus* TRB3$^{-/-}$ mice. Prior to assessing insulin-stimu-

lated activation of AKT kinase, islets pooled from multiple WT or TRB3$^{-/-}$ mice were cultured in KRBH buffer (without serum or glucose) for 2 h to minimize insulin secretion and autocrine insulin signaling. In the absence of stimulation, phospho-AKT levels drop rapidly, most likely due to net increase in phosphatase activity. Incubation in KRBH was followed by a short 10-min stimulation with insulin and Western blots of islet protein extracts were examined for AKT activation using phospho-AKT-Thr-308 and phospho-AKT-Ser-473 specific antibodies. Total AKT levels were used as control. WT islets showed a strong, insulin-stimulated induction of AKT phosphorylation at both Thr-308 and Ser-473 sites (Fig. 1*B*). TRB3$^{-/-}$ islets displayed high basal AKT phosphorylation, even under fasting conditions. Insulin stimulation did not induce a significant change in AKT phosphorylation beyond that seen under basal conditions in TRB3$^{-/-}$ islets (Fig. 1, *B* and *C*). These data suggest that in the absence of TRB3, dephosphorylation of AKT may be diminished.

We next examined how the absence of TRB3 impacts the proinflammatory signaling response in islets. To this end, we pooled islets from multiple mice within the WT and TRB3 knock-out groups, treated the islets with IL-1β, and examined time-dependent MLK3 induction and JNK activation. Under unstimulated conditions, both groups showed little or no expression of MLK3 (Fig. 1*D*, *lanes 9* and *10*). Western blotting of cytokine-treated islets pooled from TRB3 null mice show a blunted and shorter induction of MLK3 protein levels compared with that in WT islets. Peak MLK3 induction in TRB3$^{-/-}$ islets was ~3–4-fold lower than WT islets (compare *lanes 1* and *2* with *lane 6*). MLK3 expression began to taper off by 60 min in TRB3$^{-/-}$ islets (*lanes 7* and *8*), whereas WT islets showed persistence of MLK3 expression even at 5 h post-stimulus (*lanes 3* and *4*). Consistent with its role as a MAP3K that initiates cytokine-mediated JNK activation, the pattern of MLK3 induction was reflected in the time-dependent activation of phospho-JNK, with a similarly attenuated response in TRB3$^{-/-}$ islets compared with WT islets. Again, JNK activation in WT islets persisted beyond that seen in TRB3$^{-/-}$ islets. Densitometric analyses of Western blots from time courses of cytokine-treated islets were graphed and used to measure area under the curve to assess total MLK3 and JNK activation. Average area under the curve measurements from three experiments show sharply lower induction of both MLK3 and JNK in TRB3$^{-/-}$ islets (Fig. 1*E*).

Results from Fig. 1, *B–E*, suggest that a loss of TRB3 expression and/or an associated increase in AKT activation determine the course of MLK3 induction. We therefore performed the converse experiment and asked whether AKT inhibition could augment IL-1β-mediated MLK3 induction. Min6 insulinoma cells were treated with IL-1β in the presence and absence of an AKT-inhibiting compound and examined for endogenous MLK3 expression. As seen in Fig. 1*F*, a short (30-min) preinhibition of AKT did not induce a discernable basal expression of MLK3 protein, but prior inhibition of AKT was sufficient to potentiate IL-1β-mediated induction of MLK3 (see densitometric analysis in Fig. 1*G*).

To examine whether TRB3 directly contributes to the dampening effect of AKT on MLK3 levels, we transfected Min6 cells with equal amounts of GST-MLK3 in the presence of kinase dead or constitutively active myristoylated AKT. Despite equal transfection, compared with AKT-KD (Fig. 1*H*, *lane 1*), expression of MLK3 was strongly reduced in the presence of myristoylated AKT (*lane 2*). Increasing expression of TRB3 restored and augmented MLK3 expression (*lanes 3* and *4*) nearly 2-fold, suggesting that MLK3 levels are sustained by TRB3-dependent inhibition of AKT.

AKT-mediated Phosphorylation Destablizes MLK3 Protein—We have previously reported that MLK3-TRB3 binding enhances levels of both proteins, indicating that TRB3 could both inhibit AKT and stabilize MLK3. To examine whether AKT could directly regulate MLK3 protein stability, GST-MLK3 fusion constructs were expressed in Min6 insulinoma cells and subjected to a cycloheximide chase in the absence or presence of AKT inhibitor. Experiments were conducted in regular growth medium, which maintains AKT activation due to autocrine effects of insulin. Western blots of GST pulldowns were assessed for total MLK3 protein levels using anti-GST antibodies. Results from these experiments showed increased, time-dependent loss of MLK3 in cells treated with insulin (Fig. 2*A*, *lanes 5–7*), whereas addition of an AKT inhibitor markedly attenuated this loss of MLK3 (*lanes 2–4*). A graph showing the densitometric quantification of total MLK3 levels at each point clearly demonstrated a 4–5-fold drop in the half-life of MLK3, down to 25 min in the presence of insulin, *versus* 100–120 min in the presence of insulin and AKT inhibitor (Fig. 2*B*).

A previous study has reported that AKT directly interacts with and inhibits MLK3 action possibly as a consequence of C-terminal serine 674 (Ser-674) phosphorylation (27). However, the biologic context and mechanism for phospho-Ser-674-mediated suppression of MLK3 activity remains to be defined. We therefore examined whether MLK3 was phosphorylated in response to insulin stimulation in beta cell lines. GST-MLK3-transfected Min6 cells were maintained in 3 mM glucose medium for 4 h and treated with insulin in the presence or absence of AKT inhibitor, and GST pulldowns were subjected to Western blotting using AKT, phosphosubstrate-specific antibodies. These antibodies recognize AKT kinase substrates with conserved arginine residues in the −3 and −5 positions (*RXRXX*(pS/pT)) of the phosphorylation site. Using these antibodies, we observed GST-MLK3 phosphorylation in response to insulin, which was lost upon treatment with AKT inhibitor (Fig. 2*C*).

Although the comparison of MLK3 protein sequences revealed 94–99% identity across multiple mammalian species, the aforementioned AKT phosphorylation site at Ser-674 was poorly conserved (Fig. 2*D*). A closer examination identified an additional, broadly conserved consensus motif for AKT phosphorylation, located at threonine 477 (Thr-477), immediately adjacent to the leucine zipper homodimerization domain of MLK3 protein. We examined AKT-mediated MLK3 phosphorylation by an *in vitro* kinase assay using purified AKT kinase and GST fusion proteins of MLK3-WT or MLK3 bearing point mutations in each of the AKT consensus sites, individually or combined. As seen in Fig. 2*E*, matched levels of GST-MLK3 fusion proteins were incubated with [γ^{32}P]ATP in the absence or presence of purified AKT kinase. The MLK3 inhibitor

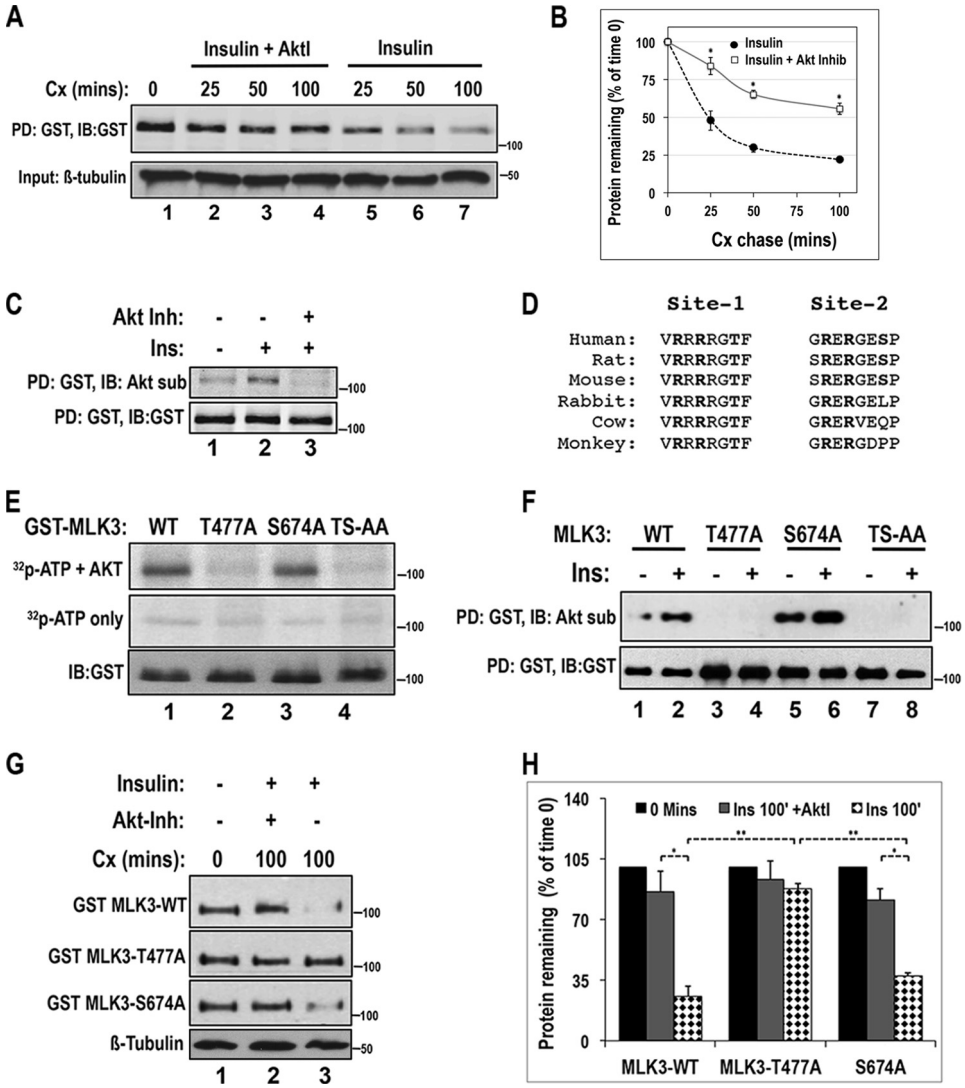

FIGURE 2. **AKT phosphorylates and regulates MLK3 stability.** *A*, time-dependent cycloheximide (*Cx*) chase of GST-MLK3 from Min6 cells treated with insulin in the presence (*lanes 2–4*) and absence (*lanes 5–7*) of an AKT kinase inhibitor (*Inhib* or *Inh*) followed by GST pulldown (*PD*) assays and Western blotting (*IB*) using anti-GST antibodies. Cellular inputs were probed for β-tubulin control. *B*, densitometric quantification of time-dependent loss of MLK3 protein from three independent experiments shown as mean protein remaining ± S.E. demonstrate a 4–5-fold drop in the stability of GST-MLK3 in the presence of insulin ($t_{1/2}$ = 25 min), but not in the presence of AKT inhibitor ($t_{1/2}$ = 120 min). *, $p < 0.001$ *versus* insulin treatment in the absence of AKT inhibitor. *C*, AKT-dependent phosphorylation of GST-MLK3 in Min6 cells treated with insulin for 20 min (*lanes 2* and *3*) in the absence (*lanes 1* and *2*) or presence (*lane 3*) of AKT kinase inhibitor. GST pulldowns were probed with an AKT substrate-specific antibody. Total levels of GST-MLK3 are shown. *D*, identification of AKT consensus sites 1 and 2 in the sequence human (*top*) of MLK3 protein. Only site 1 was conserved across all mammalian species examined. *E*, *in vitro* phosphorylation of purified GST-MLK3 WT (*lane 1*) or AKT consensus mutants GST-MLK3 T477A, S674A (*lanes 2–4*), was performed using recombinant AKT kinase and γ^{32}p-ATP, followed by SDS-PAGE and autoradiography. Equal levels of starting material were determined using anti-GST Western blotting. *F*, insulin-induced (20 mins) *in vivo* phosphorylation of MLK3 proteins was assessed using pulldowns of GST-MLK3 fusion proteins expressed in Min6 cells. AKT substrate-specific antibodies detected phosphorylation of GST-MLK3 WT (WT) (*lanes 1* and *2*) and S674A (*lanes 5* and *6*), but no signal was observed for T477A, or the TS-AA mutants (*lanes 3* and *4* and *lanes 7* and *8*, respectively). *G*, stability of the GST-MLK3 WT and AKT consensus mutants T447A and S674A was assessed using GST pulldowns expressed in Min6 cells treated with insulin and cycloheximide for 100 min (*lane 1*, time 0) in the presence (*lane 2*) or absence of AKT inhibitor (*lane 3*) as indicated. No appreciable time-dependent loss was observed for a more stable protein similar to β-tubulin. *H*, densitometric analyses of MLK3 protein levels under conditions described in *G* are presented in a bar graph, and show mean values ± S.E. of three separate experiments. *, $p < 0.01$ *versus* insulin treatment in the presence of AKT inhibitor and ** $p < 0.01$ *versus* insulin (*Ins*) treated MLK3 WT and S674A mutant.

CEP11004 was included in the assay to prevent autophosphorylation. Under these conditions, AKT kinase robustly phosphorylated GST-MLK3-WT, as well as alanine (Ala) substitution mutant at Ser-674 (GST-MLK3-S674A). MLK3 constructs with an alanine substitution mutation at Thr-477 (GST-MLK3-T477A) failed to undergo AKT-dependent phosphorylation *in vitro*.

Results from Fig. 2*E* prompted us to examine whether AKT also favored phosphorylation of Thr-477 *in vivo*. Again, the cells were starved in low glucose, and the samples were analyzed as described for Fig. 2*C*. Similar to results from *in vitro* kinase assays, we found that insulin stimulation resulted in phosphorylation of MLK3 at Thr-477 but not Ser-674 (Fig. 2*F*). Thus, under conditions used in this study, AKT preferentially phosphorylates MLK3 at a novel site both *in vitro* and in Min6 cells *in vivo*.

We next examined whether AKT-dependent loss of MLK3 protein stability required phosphorylation at Thr-477. Min6

cells expressing WT, T477A, or S674A mutants of GST-MLK3 were treated with cycloheximide and insulin in the presence or absence of AKT inhibitor. Cells were harvested prior to the insulin stimulus to mark basal levels of MLK3 protein expression at time 0 and at 100 min following insulin treatment. Western blots of the GST pulldowns showed that AKT inhibitor prevented the loss of MLK3 protein, regardless of the mutation (Fig. 2*G*, *lanes 1* and *2*). However, insulin treatment in the absence of AKT inhibitor markedly decreased (≈60%) levels of both MLK3-WT and S674A mutant but had no effect on levels of T477A mutant of MLK3 (*lane 3*). Inputs from all samples were probed for the more stable β-tubulin protein used here as a control (half-life of 50 h (28)). A representative panel with comparable levels of β-tubulin from GST-MLK3-WT input samples was shown. Total protein levels at each time point were densitometrically assessed and an average of three experiments was graphically represented in Fig. 2*H*.

Thr-477 Phosphorylation Triggers Lys-48-linked Polyubiquitination of MLK3—Tandem phosphorylation and polyubiquitination are well characterized post-translational modifications for targeting the proteasomal clearance of cellular proteins. We examined whether MLK3 is targeted to the proteasome in response to insulin. We have previously shown that cytokine-stimulation activates MLK3 via TRAF6-dependent Lys-63-linked polyubiquitination (14). Lys-48-linked polyubiquitin chains target proteins toward proteasomal breakdown prompting us to examine insulin-induced Lys-63-independent polyubiquitination of MLK3 (Fig. 3*A*). GST-MLK3 was co-expressed with Lys-63 (Myc-Ub-K63R) mutant or Lys-48 (Myc-Ub-K48R) mutants of Myc-tagged ubiquitin, the cells briefly stimulated with insulin in the presence of the proteasome inhibitor MG132, and ubiquitination of GST-MLK3 pulldowns was assessed using anti-Myc antibodies. Insulin increased ubiquitination of MLK3 in the presence of Ub-K63R, but MLK3 polyubiquitination was abolished upon usage of ubiquitin-K48R mutant. To avoid confusion with Lys-63-linked ubiquitination, all subsequent experiments examining insulin-induced ubiquitination were conducted using Myc-Ub-K63R. We next examined whether insulin-mediated polyubiquitination of MLK3 requires AKT-dependent prephosphorylation. Min6 cells expressing GST-MLK3-WT or GST-MLK3-T477A were briefly treated with insulin in the presence of MG132, and Western blots of GST pulldowns were probed with anti-Myc antibodies. As seen in Fig. 3*B*, MLK3-WT was polyubiquitinated in response to insulin (*lanes 1* and *2*), and mutation of Thr-477 (*lanes 3* and *4*) resulted in a marked loss of the Myc-ubiquitin signal. Thus, AKT-mediated phosphorylation is required for insulin-stimulated MLK3 ubiquitination.

Insulin Destabilizes MLK3 via Lys-48-linked Ubiquitination of MLK3 at Lysine 264—Using an experimental design similar to that in Fig. 3*B*, we localized insulin-dependent Lys-48-linked ubiquitination to the N-terminal half of MLK3, which harbors the catalytic domain of this kinase. As seen in Fig. 3*C*, compared with MLK3-WT, deletion of the first 400 amino acids (Δ400) induced a marked attenuation of insulin-stimulated MLK3 ubiquitination. Using identical experimental conditions to those in Fig. 3, *B* and *C*, we sought to map the ubiquitin acceptor site in MLK3 protein. Lysine to arginine (Lys-to-Arg) substitution mutants of residues in the catalytic domain of MLK3 were assessed for insulin-induced polyubiquitination. In the absence of a clear known consensus site for Lys-48-linked ubiquitination, we first screened previously generated mutants used for mapping Lys-63-linked ubiquitination of MLK3 (14). Arginine substitution mutants of MLK3 at Lys-130, Lys-180, and Lys-264, were used in GST pulldown experiments followed by anti-Myc Western blots. Whereas insulin treatment induced ubiquitination of MLK3-WT, K130R, and K180R constructs, the K264R (*lanes 7* and *8*) mutation abolished insulin-stimulated ubiquitination of MLK3. Based on the widely accepted role of Lys-48-linked polyubiquitination in protein degradation, the K264R mutant of MLK3 would be expected to resist insulin-stimulated degradation. As shown in Fig. 3*E*, we found that irrespective of the presence of insulin or an AKT inhibitor, MLK3-K264R did not show a significant change in protein levels (Fig. 3*E*, *lanes 1–3*). By contrast, insulin treatment resulted in >60% degradation of wild-type MLK3 protein, and this steep loss was prevented by the presence of an AKT inhibitor (*lanes 4–6*). Inputs were probed for β-tubulin used here as control. A bar graph representing results from three independent experiments is shown in Fig. 3*F*. For direct comparison, cycloheximide chase experiments using MLK3-WT, T477A, S674A, phospho-mutants (Fig. 2*G*) were performed along with K264R ubiquitin mutant (Fig. 3*E*). However, for a clearer description of the results, these data have been represented in two independent figures. We conclude that AKT regulates MLK3 protein stability by targeting phosphorylation (Fig. 2*G*) and subsequent ubiquitination (Fig. 3*E*).

Although the ubiquitin acceptor mutant of MLK3 appears to be more stable, Fig. 3*E* revealed noticeably faster migration of MLK3-K264R. The significance of a faster migrating MLK3-K264R mutant can be explained by our previous report showing IL-1β-stimulated, Lys-63-linked ubiquitination at Lys-264 (see schematic in Fig. 3*G*) (14). Because Lys-63-linked ubiquitination aids the dimerization, autophosphorylation, and activation of MLK3, mutation of Lys-264 also renders MLK3 inactive. As shown in Fig. 3*H*, we transfected GST-MLK3-WT, KD, or K264R mutants of MLK3 into Min6 cells along with GST-JNK (to distinguish from faster migrating endogenous JNK) and used the extracts for GST pulldowns followed by Western blotting for JNK phosphorylation. Consistent with the literature, and unlike MLK3-KD (*lane 2*), MLK3-WT expression was sufficient to induce autophosphorylation, as well as the phosphorylation of JNK (*lane 3*). A brief treatment of the cells with MLK inhibitor CEP11004 rapidly inhibited phosphorylation of MLK3 and GST-JNK (*lane 4*), whereas the K264R mutant of MLK3 was inactive and showed no JNK phosphorylation and minimal autophosphorylation. Taken together, these data clearly demonstrate that AKT regulates MLK3 by precluding activation-specific Lys-63-linked ubiquitination, while stimulating phosphorylation-dependent ubiquitination and proteasomal degradation.

Mutation of AKT Phospho-acceptor Site Augments Proapoptotic Properties of MLK3—We have previously demonstrated a key role for MLK3 in cytokine-induced beta cell apoptosis (6, 14). Having found that AKT destabilizes MLK3 protein, we examined whether a point mutant of MLK3 (T477A) that

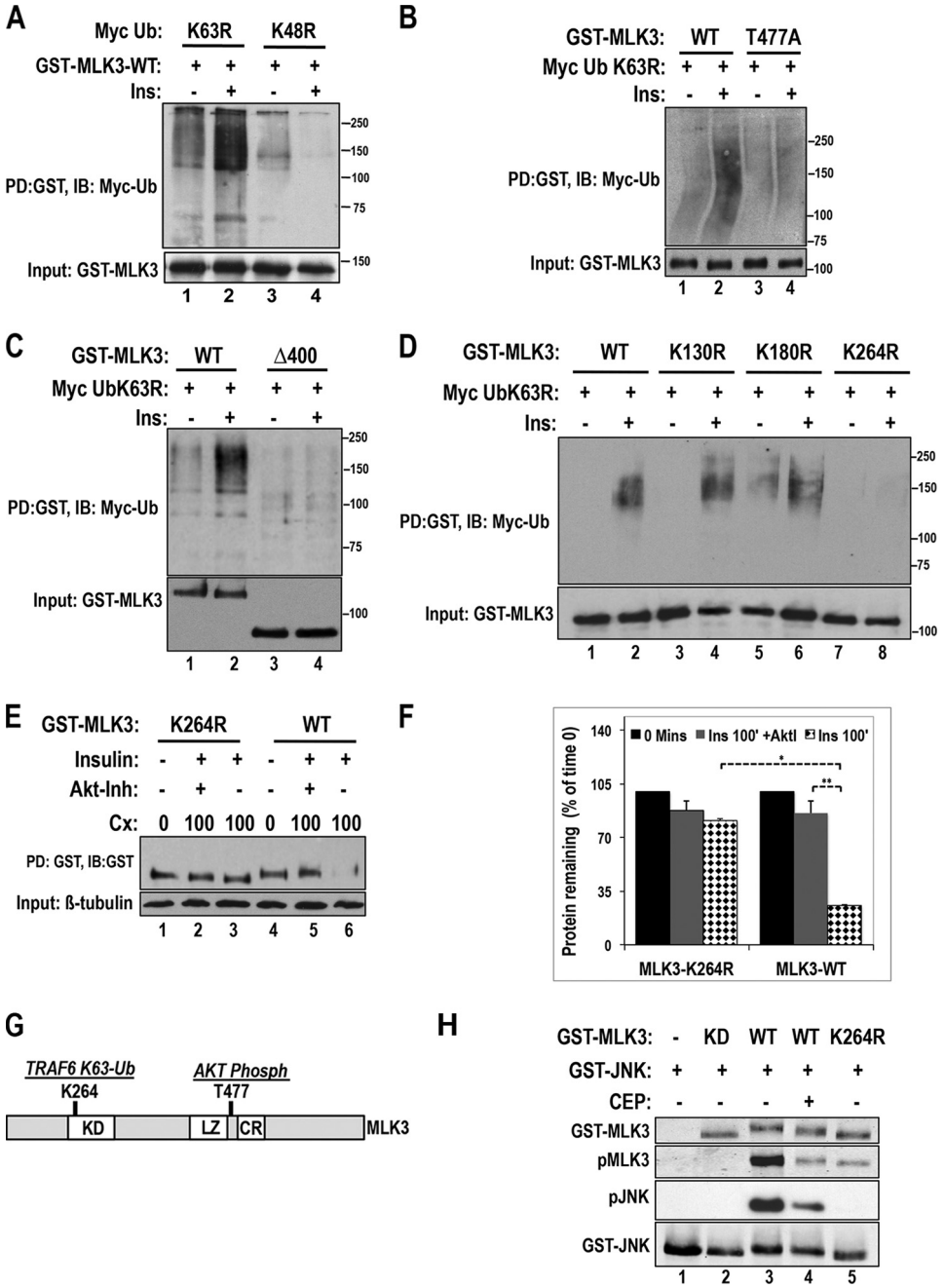

FIGURE 3. **Insulin-dependent ubiquitination of MLK3.** *A*, insulin-dependent ubiquitination of MLK3 proteins was assessed using GST pulldowns (*PD*) from Min6 cells coexpressing GST-MLK3-WT along with Myc-tagged K63R mutant of ubiquitin (*Myc-Ub-K63R*, *lanes 1* and *2*) or Myc-ubiquitin-K48R (*lanes 3* and *4*). Cells were treated with for insulin for 30 min (*lanes 2* and *4*), and Western blots using anti-Myc antibodies were to detect ubiquitination of MLK3. Total levels of MLK3 in each lane are shown. *B*, GST pulldowns of MLK3-WT or T447A mutant from cells coexpressing Myc-Ub-K63R, treated with insulin for 30 min (*lanes 2* and *4*), show loss of ubiquitination for AKT phosphomutant of MLK3. *C*, insulin-mediated MLK3 ubiquitination was observed for GST-MLK3 WT but not for the N-terminal deletion of MLK3 (Δ400) using experimental conditions described in *B*. *D*, site-specific mutants of potential ubiquitin acceptor lysine residues in GST-MLK3 were examined for insulin-dependent ubiquitination as described in *A* and show specific loss of ubiquitination upon mutation of Lys-264 in MLK3 protein. *E*, autoradiogram showing time-dependent, insulin-mediated loss of GST-MLK3 WT (*lanes 4–6*), but not GST-MLK3 K264R (*lanes 1–3*). Total MLK3 protein levels from untreated cells at time 0 are shown in *lanes 1* and *4*, whereas MLK3 levels from cycloheximide (*Cx*)-treated cells in the presence (*lanes 2* and *4*) or absence of (*lanes 3* and *6*) AKT inhibitor are shown. Note that for a direct comparison, experiments on stability of GST-MLK3 K264R were performed alongside corresponding MLK3 phospho-mutants T477 A and S674A (Fig. 2*G*). *F*, densitometric analysis MLK3 protein stability using conditions described in *E* are presented as a bar graph and represent means ± S.E. of three independent experiments. *, $p < 0.01$ *versus* MLK3-WT treatment with insulin and **, $p < 0.01$ *versus* insulin (*Ins*) treatment of MLK3-WT in the presence of AKT inhibitor. *G*, schematic representation of MLK3 protein highlighting the acceptor lysine (Lys-264) for TRAF6-dependent Lys-63-linked ubiquitination and the AKT phosphorylation site at Thr-477. Functional domains of the MLK3 protein include the following: kinase domain (*KD*), leucine zipper (*LZ*), and CDC42-Rac interacting CR (*CRIB* domain). *H*, functionality of MLK-ubiquitin acceptor mutant was assessed using pulldowns of GST-JNK, from HepG2 cells co-transfected with MLK3-kinase-dead (*KD*, *lane 2*), WT (*lanes 3* and *4*), and K264R mutant (*lane 5*), followed by Western blotting using phosho-JNK as well as phospho-MLK3-specific antibodies (*middle panels*). 500 nM MLK3 inhibitor Cep111004 was used as a control to demonstrate impact of MLK3 inhibition on JNK activity (*lane 4*). Total GST-MLK3 and GST-JNK input controls are shown.

escaped AKT-dependent phosphorylation could increase its proapoptotic impact. Min6 insulinoma cells were transfected with GST control vector, GST-MLK3-WT, or GST-MLK3-T477A, and cell death was assessed using TUNEL assay in the presence or absence of cytokines (mixture of TNF-α, IL-1β, and IFN-γ). In Min6 cells, we generally observed cytokine-stimulated death as early as 16 h, peaking at 24–36 h. Consistent with its role as a competence factor for beta cell apoptosis (6), MLK3-expressing cells are sensitized to the effect of cytokines, resulting in precocious cell death. To capture this accelerated time frame, MLK3-expressing cells were treated with cytokines for a sub-lethal period of 8 h. Cells were co-stained for MLK3 expression using anti-GST antibodies, and TUNEL+ cells were expressed as a percent of total transfected MLK3+ cells. In vector controls, cytokine treatment showed little change in cell death. MLK3-WT expression resulted in apoptosis of roughly 20–30% of the transfected cells, which was further augmented (2–3-fold) in the presence of cytokines. Interestingly, MLK3-T477A expression strongly induced cell death, resulting in apoptosis of nearly 60% of the transfected cells, comparable with levels observed in cytokine-treated MLK3-WT expressing cells. More importantly, unlike MLK3-WT, addition of cytokines did not further augment MLK3-T477A-induced death of Min6 cells. These data clearly indicate that MLK3-T477A is already active at a maximal level and imply that AKT is likely the main negative regulator of MLK3 under prosurvival conditions.

Loss of TRB3 Attenuates Cytokine-induced Beta Cell Death—Results shown in the preceding figure would predict that primary beta cells from TRB3$^{-/-}$ mice are resistant to cytokine-induced cell death. To examine this hypothesis, we used an *ex vivo* co-culture model intended to mimic the islet response to leukocyte invasion or insulitis associated with autoimmune type 1 diabetes. Unlike static culture of islets with cytokine cocktails, this system (depicted by a schematic in Fig. 4*B*) more authentically recapitulates the complex cytokine environment of insulitis. Splenocytes from WT mice were isolated and stimulated with plate bound anti-CD3 and anti-CD28 antibodies to trigger production of the full repertoire of cytokines as reported (6). For co-culture, isolated islets from WT or TRB3$^{-/-}$ mice were suspended in Transwells and immersed in culture wells containing stimulated or unstimulated (naïve) splenocytes. Islets were thus co-cultured for 24 h, fixed, processed, and examined for activation of cell death. We have reported previously that cytokine induced TRB3 expression in islets and beta cell lines is highly correlated with conformational alteration in BAX, a proapoptotic BH3-only protein of the BCL family of proteins (6). Conformational change is required for and immediately precedes the insertion of BAX into the outer mitochondrial membrane, as detected by a conformation-specific antibody (BAX6A7) (29, 30). BAX translocation, oligomerization, and insertion result in cytoplasmic leaching of cytochrome *c*, ultimately resulting in activation of executioner caspase-3 and induction of apoptosis (31, 32). As seen in Fig. 4*C*, under unstimulated conditions, both WT and TRB3$^{-/-}$ islets showed little or no BAX6A7 signal. Co-culture of WT islets with activated splenocytes resulted in BAX6A7 detection in ~8% of the beta cells (Fig. 4*E*). Consistent with our reported correlation between TRB3 induction and BAX conformational change, TRB3$^{-/-}$ islets showed little signal beyond an occasional BAX6A7+ beta cell.

Finally, we examined whether loss of TRB3 expression could protect beta cells from cytokine-induced apoptosis. Again using the co-culture model, we observed strong induction of cell death in WT islets (Fig. 4*D*). Quantification of TUNEL+ cells showed induction of roughly 15–25% of total insulin+ cells across multiple islets (Fig. 4*F*). In TRB3$^{-/-}$ islets, we observed a virtual absence of beta cell death, indicating that loss of TRB3 strongly protected beta cells from apoptosis.

DISCUSSION

Accumulating evidence suggests that the MLK-JNK signaling pathway induces inflammation of metabolic tissues and contributes to impaired glucose homeostasis and decreased insulin sensitivity (33–38). In the beta cell, cross-talk between MLK-JNK and insulin-AKT signaling determines the balance between dysfunction/death and survival, highlighting the importance of mechanisms that can fine tune and tip the balance toward JNK or AKT activity. We have previously shown that TRB3 is a downstream mediator of MLK3 and is required for induction of cytokine-dependent beta cell inflammation (6). Here, we show that TRB3 is instrumental in regulating the net amount of MLK3 available for participating in JNK signaling, most likely by inhibiting AKT and preventing AKT-mediated proteasomal degradation of MLK3. Thus, TRB3 functions as an allosteric modulator that fine-tunes the inverse balance between MLK3 and AKT in cytokine-induced beta cell inflammation.

In the beta cell, autocrine insulin action resulting from periodic glucose-stimulated insulin secretion (25, 26) is sufficient to maintain the prosurvival effects of AKT. Mice with beta cell-specific deletion of both insulin and IGF1 receptors show profound loss of AKT activity, extensive beta cell death and severe diabetes (39). Similar phenotypes have been reported in mice with a global knock-out of AKT2 (40), and genetic ablation of IRS2 (insulin receptor substrate 2) (41). Additionally, incretins mediate their potent prosurvival effects at least in part by inducing IRS2 expression and subsequent AKT activation (42, 43). AKT-dependent regulation of protein stability can be mediated by direct phosphorylation of substrates, as is the case with tuberin, FOXO3, and FOXO1 (44, 45). However, AKT also indirectly regulates protein stability via GSK3 to impact beta cell function and survival. GSK3-mediated phosphorylation and proteasomal degradation is a prevalent mechanism (46) and reportedly regulates beta-cell specific transcription factors PDX1 (47, 48) and MAF-A (49, 50), as well as MCL-1 (51, 52), an antiapoptotic BCL family protein.

In addition to the cross-talk between post-translational events of phosphorylation and ubiquitination, this study illustrates how cross-talk between two distinct types of ubiquitination events can control MLK3 function and stability. We have shown that IL-1β/TRAF6 activates MLK3 by atypical Lys-63-linked ubiquitination of Lys-264. Others have also reported both Lys-63- and Lys-48-linked ubiquitination of MLK3 (12, 13), but the relevance to specific biological conditions has not been established. In this report, we clarify that competing Lys-

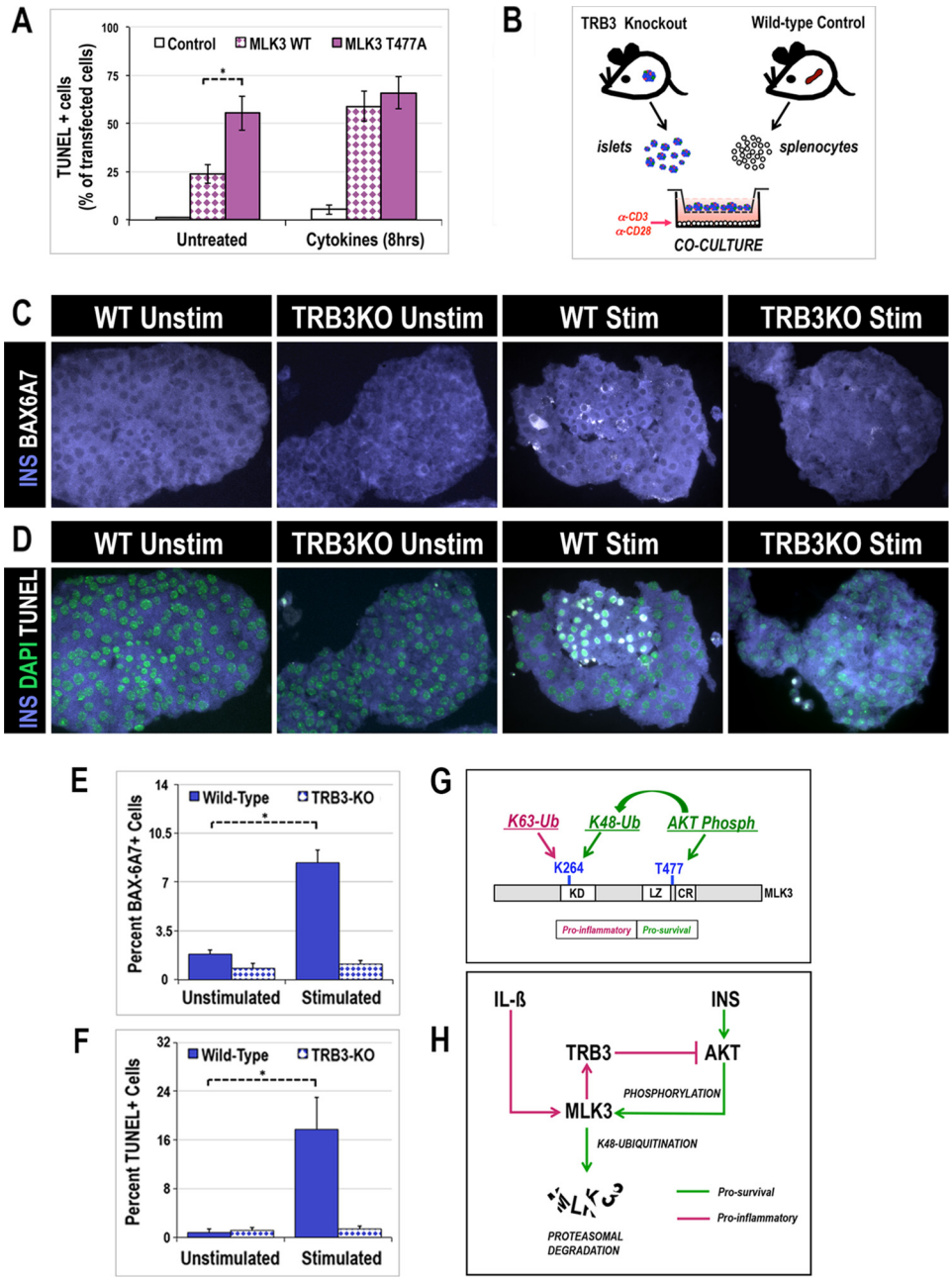

FIGURE 4. **Loss of AKT-mediated MLK3 phosphorylation potentiates, whereas genetic ablation of TRB3 protects beta cells from cytokine induced cell death.** *A*, MLK3-T477A-induced increase in TUNEL positive Min6 cells under basal conditions compared with either MLK3-WT or vector control. Cytokine 8-h treatment of vehicle alone (*Untreated*) or a cytokine mixture of 10 nM TNF-α, 40 ng/ml IFN-γ, and 20 ng/ml IL-1β, augmented MLK3-WT-induced cell death, whereas no further increase was observed in the presence of MLK3-T477A. *, $p < 0.05$ *versus* MLK3-WT in untreated cells. (Primary data included in supplemental Fig. 2.) *B*, schematic representation of splenocyte islet co-culture experimental model used for examination of beta cell death. *C*, BAX conformational change was examined in WT and TRB3-KO islets following 24 h of splenocyte and islet co-culture using unstimulated (*Unstim*) or stimulated (*Stim*) splenocytes. Immunofluorescence using insulin (pseudocolored *blue*) and BAX6A7 conformation-specific antibodies (pseudocolored *white* for clarity) show stimulation-dependent induction of BAX conformational change in WT islets but not in TRB3-KO islets. *D*, sections generated from the splenocyte and islet co-culture experiments in *C* were also processed and examined for insulin along with induction of death by TUNEL assay (pseudocolored *white*). Similar to data seen for BAX6A7, TRB3-KO islets show marked attenuation of cell death. Nuclei were counterstained with DAPI (shown in *C* only). *E* and *F*, quantification of BAX-6A7 and TUNEL-positive beta cells is shown in bar graphs and represent the mean ± S.E. of three separate experiments. *, $p < 0.01$ *versus* WT islets cultured with unstimulated splenocytes. *G* and *H*, schematic representation of post-translational modifications of MLK3 (*G*) and a working model for the cross-talk between MLK3, TRB3, and AKT based on the findings shown in the current study (*H*).

48- and Lys-63-linked ubiquitination events not only regulate the fate of the MLK3 molecule but likely also impact survival of the beta cell. The fact that both ubiquitination events can target the same lysine (Lys-264) residue in the kinase domain of MLK3 underscores the tight regulatory controls on MLK3 (depicted by a model in Fig. 4*G*) and thereby the importance of MLK3 in beta cell inflammation and death.

Despite the presence of multiple families of MAP3Ks, cytokines appear to signal via a fairly specific JNK signaling module that includes MLK3, MKK7/4, and JNK1, scaffolded by JIP1

(15–17). We have reported that TRAF6-mediated, Lys-63-linked ubiquitination induces MLK3 dissociation from JIP1 scaffold, enabling its dimerization and activation of the MLK3-JNK cascade (14). Furthermore, JNK activation is sustained by direct phosphorylation of JIP1, which inhibits re-association of MAP3Ks with JIP1 (53). Notably, Xu *et al.* (18) have demonstrated that upon cytokine treatment, each component of the JNK activation cascade contributes to the mutual stabilization of the entire module sustaining a feed-forward loop of MLK3-MKK7 and JNK activation. This report shows that TRB3 is required for optimal dynamics of JNK signaling such that loss of TRB3 decreases both the amplitude and duration of MLK3-JNK activation. In neurons, duration of MLK-JNK signaling is regulated by a negative feedback mechanism, in which dephosphorylation of JNK is induced by Jun/AP1 induced expression of MAP kinase phosphatase 1 (54). By contrast, a drop in total MLK3 protein levels could explain a decrease in both the amplitude and duration of JNK activation. As depicted in Fig. 4*H*, we propose that in the absence of TRB3, increased AKT activity could rapidly induce MLK3 degradation, decreasing total amounts of MLK3 available for JNK activation.

Results presented in this study show that a change in kinetics of MLK3-JNK activation can impact beta cell inflammation and survival. Downstream biological effects resulting from shifts in signaling dynamics may not be uniform (55, 56) and could be likened to continuous analog *versus* discrete digital outputs. For example, increase or decrease in kinase signaling may result in a proportional shift in downstream effects. Alternately, a specific amplitude and duration of signaling may be required for attaining a signaling threshold, triggering a discrete switch-like "all or nothing" response (discussed in Ref. 57).

Thus, in addition to signal-dependent activation of distinct pathways and kinase isoforms, signaling agonists may elicit specific biologic responses via the information encoded within the dynamics of signal activation (57). It would follow, therefore, that in beta cells, the downstream impact of TRB3-dependent allosteric fine-tuning of signaling mechanisms could be complex and nuanced and merits further inquiry.

REFERENCES

1. Cnop, M., Welsh, N., Jonas, J. C., Jörns, A., Lenzen, S., and Eizirik, D. L. (2005) Mechanisms of pancreatic β-cell death in type 1 and type 2 diabetes: many differences, few similarities. *Diabetes* **54,** S97–107
2. Donath, M. Y., Dalmas, É., Sauter, N. S., and Böni-Schnetzler, M. (2013) Inflammation in obesity and diabetes: islet dysfunction and therapeutic opportunity. *Cell Metab.* **17,** 860–872
3. Novotny, G. W., Lundh, M., Backe, M. B., Christensen, D. P., Hansen, J. B., Dahllöf, M. S., Pallesen, E. M., and Mandrup-Poulsen, T. (2012) Transcriptional and translational regulation of cytokine signaling in inflammatory β-cell dysfunction and apoptosis. *Arch. Biochem. Biophys.* **528,** 171–184
4. Perier, C., Bové, J., Wu, D. C., Dehay, B., Choi, D. K., Jackson-Lewis, V., Rathke-Hartlieb, S., Bouillet, P., Strasser, A., Schulz, J. B., Przedborski, S., and Vila, M. (2007) Two molecular pathways initiate mitochondria-dependent dopaminergic neurodegeneration in experimental Parkinson's disease. *Proc. Natl. Acad. Sci. U.S.A.* **104,** 8161–8166
5. Putcha, G. V., Le, S., Frank, S., Besirli, C. G., Clark, K., Chu, B., Alix, S., Youle, R. J., LaMarche, A., Maroney, A. C., and Johnson, E. M., Jr. (2003) JNK-mediated BIM phosphorylation potentiates BAX-dependent apoptosis. *Neuron* **38,** 899–914
6. Humphrey, R. K., Newcomb, C. J., Yu, S. M., Hao, E., Yu, D., Krajewski, S., Du, K., and Jhala, U. S. (2010) Mixed lineage kinase-3 stabilizes and functionally cooperates with TRIBBLES-3 to compromise mitochondrial integrity in cytokine-induced death of pancreatic beta cells. *J. Biol. Chem.* **285,** 22426–22436
7. Sabio, G., and Davis, R. J. (2014) TNF and MAP kinase signalling pathways. *Semin. Immunol.* **26,** 237–245
8. Kyriakis, J. M., and Avruch, J. (2012) Mammalian MAPK signal transduction pathways activated by stress and inflammation: a 10-year update. *Physiol. Rev.* **92,** 689–737
9. Haglund, K., and Dikic, I. (2005) Ubiquitylation and cell signaling. *EMBO J.* **24,** 3353–3359
10. Pineda, G., Ea, C. K., and Chen, Z. J. (2007) Ubiquitination and TRAF signaling. *Adv. Exp. Med. Biol.* **597,** 80–92
11. Sun, L., and Chen, Z. J. (2004) The novel functions of ubiquitination in signaling. *Curr. Opin. Cell Biol.* **16,** 119–126
12. Korchnak, A. C., Zhan, Y., Aguilar, M. T., and Chadee, D. N. (2009) Cytokine-induced activation of mixed lineage kinase 3 requires TRAF2 and TRAF6. *Cell Signal.* **21,** 1620–1625
13. Sondarva, G., Kundu, C. N., Mehrotra, S., Mishra, R., Rangasamy, V., Sathyanarayana, P., Ray, R. S., Rana, B., and Rana, A. (2010) TRAF2-MLK3 interaction is essential for TNF-α-induced MLK3 activation. *Cell Res.* **20,** 89–98
14. Humphrey, R. K., Yu, S. M., Bellary, A., Gonuguntla, S., Yebra, M., and Jhala, U. S. (2013) Lysine 63-linked ubiquitination modulates mixed lineage kinase-3 interaction with JIP1 scaffold protein in cytokine-induced pancreatic beta cell death. *J. Biol. Chem.* **288,** 2428–2440
15. Tournier, C., Dong, C., Turner, T. K., Jones, S. N., Flavell, R. A., and Davis, R. J. (2001) MKK7 is an essential component of the JNK signal transduction pathway activated by proinflammatory cytokines. *Genes Dev.* **15,** 1419–1426
16. Whitmarsh, A. J., Cavanagh, J., Tournier, C., Yasuda, J., and Davis, R. J. (1998) A mammalian scaffold complex that selectively mediates MAP kinase activation. *Science* **281,** 1671–1674
17. Whitmarsh, A. J., Kuan, C. Y., Kennedy, N. J., Kelkar, N., Haydar, T. F., Mordes, J. P., Appel, M., Rossini, A. A., Jones, S. N., Flavell, R. A., Rakic, P., and Davis, R. J. (2001) Requirement of the JIP1 scaffold protein for stress-induced JNK activation. *Genes Dev.* **15,** 2421–2432
18. Xu, Z., Kukekov, N. V., and Greene, L. A. (2005) Regulation of apoptotic c-Jun N-terminal kinase signaling by a stabilization-based feed-forward loop. *Mol. Cell. Biol.* **25,** 9949–9959
19. Zeqiraj, E., and van Aalten, D. M. (2010) Pseudokinases-remnants of evolution or key allosteric regulators? *Curr. Opin. Struct. Biol.* **20,** 772–781
20. Okamoto, H., Latres, E., Liu, R., Thabet, K., Murphy, A., Valenzeula, D., Yancopoulos, G. D., Stitt, T. N., Glass, D. J., and Sleeman, M. W. (2007) Genetic deletion of Trb3, the mammalian *Drosophila tribbles* homolog, displays normal hepatic insulin signaling and glucose homeostasis. *Diabetes* **56,** 1350–1356
21. Du, K., Herzig, S., Kulkarni, R. N., and Montminy, M. (2003) TRB3: a tribbles homolog that inhibits Akt/PKB activation by insulin in liver. *Science* **300,** 1574–1577
22. Kato, S., and Du, K. (2007) TRB3 modulates C2C12 differentiation by interfering with Akt activation. *Biochem. Biophys. Res. Commun.* **353,** 933–938
23. He, L., Simmen, F. A., Mehendale, H. M., Ronis, M. J., and Badger, T. M. (2006) Chronic ethanol intake impairs insulin signaling in rats by disrupting Akt association with the cell membrane. *J. Biol. Chem.* **281,** 11126–11134
24. Salazar, M., Carracedo, A., Salanueva, I. J., Hernández-Tiedra, S., Lorente, M., Egia, A., Vázquez, P., Blázquez, C., Torres, S., García, S., Nowak, J., Fimia, G. M., Piacentini, M., Cecconi, F., Pandolfi, P. P., González-Feria, L., Iovanna, J. L., Guzmán, M., Boya, P., and Velasco, G. (2009) Cannabinoid action induces autophagy-mediated cell death through stimulation of ER stress in human glioma cells. *J. Clin. Invest.* **119,** 1359–1372
25. Aikin, R., Hanley, S., Maysinger, D., Lipsett, M., Castellarin, M., Paraskevas, S., and Rosenberg, L. (2006) Autocrine insulin action activates Akt and increases survival of isolated human islets. *Diabetologia* **49,** 2900–2909
26. Assmann, A., Ueki, K., Winnay, J. N., Kadowaki, T., and Kulkarni, R. N. (2009) Glucose effects on β-cell growth and survival require activation of

insulin receptors and insulin receptor substrate 2. *Mol. Cell. Biol.* **29,** 3219–3228
27. Barthwal, M. K., Sathyanarayana, P., Kundu, C. N., Rana, B., Pradeep, A., Sharma, C., Woodgett, J. R., and Rana, A. (2003) Negative regulation of mixed lineage kinase 3 by protein kinase B/AKT leads to cell survival. *J. Biol. Chem.* **278,** 3897–3902
28. Wang, Y., Tian, G., Cowan, N. J., and Cabral, F. (2006) Mutations affecting β-tubulin folding and degradation. *J. Biol. Chem.* **281,** 13628–13635
29. Nechushtan, A., Smith, C. L., Hsu, Y. T., and Youle, R. J. (1999) Conformation of the Bax C-terminus regulates subcellular location and cell death. *EMBO J.* **18,** 2330–2341
30. Suzuki, M., Youle, R. J., and Tjandra, N. (2000) Structure of Bax: coregulation of dimer formation and intracellular localization. *Cell* **103,** 645–654
31. Finucane, D. M., Bossy-Wetzel, E., Waterhouse, N. J., Cotter, T. G., and Green, D. R. (1999) Bax-induced caspase activation and apoptosis via cytochrome c release from mitochondria is inhibitable by Bcl-xL. *J. Biol. Chem.* **274,** 2225–2233
32. Jürgensmeier, J. M., Xie, Z., Deveraux, Q., Ellerby, L., Bredesen, D., and Reed, J. C. (1998) Bax directly induces release of cytochrome c from isolated mitochondria. *Proc. Natl. Acad. Sci. U.S.A.* **95,** 4997–5002
33. Jaeschke, A., and Davis, R. J. (2007) Metabolic stress signaling mediated by mixed-lineage kinases. *Mol. Cell* **27,** 498–508
34. Kant, S., Barrett, T., Vertii, A., Noh, Y. H., Jung, D. Y., Kim, J. K., and Davis, R. J. (2013) Role of the mixed-lineage protein kinase pathway in the metabolic stress response to obesity. *Cell Rep.* **4,** 681–688
35. Jiang, J. X., and Török, N. J. (2014) MLK3 as a regulator of disease progression in NASH. *Liver Int.* **34,** 1131–1132
36. Sharma, M., Urano, F., and Jaeschke, A. (2012) Cdc42 and Rac1 are major contributors to the saturated fatty acid-stimulated JNK pathway in hepatocytes. *J. Hepatol.* **56,** 192–198
37. Ibrahim, S. H., Gores, G. J., Hirsova, P., Kirby, M., Miles, L., Jaeschke, A., and Kohli, R. (2013) Mixed lineage kinase 3 deficient mice are protected against the high fat high carbohydrate diet-induced steatohepatitis. *Liver Int.* 10.1111/liv.12353
38. Gadang, V., Kohli, R., Myronovych, A., Hui, D. Y., Perez-Tilve, D., and Jaeschke, A. (2013) MLK3 promotes metabolic dysfunction induced by saturated fatty acid-enriched diet. *Am. J. Physiol. Endocrinol. Metab.* **305,** E549–556
39. Ueki, K., Okada, T., Hu, J., Liew, C. W., Assmann, A., Dahlgren, G. M., Peters, J. L., Shackman, J. G., Zhang, M., Artner, I., Satin, L. S., Stein, R., Holzenberger, M., Kennedy, R. T., Kahn, C. R., and Kulkarni, R. N. (2006) Total insulin and IGF-I resistance in pancreatic β cells causes overt diabetes. *Nat. Genet.* **38,** 583–588
40. Garofalo, R. S., Orena, S. J., Rafidi, K., Torchia, A. J., Stock, J. L., Hildebrandt, A. L., Coskran, T., Black, S. C., Brees, D. J., Wicks, J. R., McNeish, J. D., and Coleman, K. G. (2003) Severe diabetes, age-dependent loss of adipose tissue, and mild growth deficiency in mice lacking Akt2/PKB β. *J. Clin. Invest.* **112,** 197–208
41. Withers, D. J., Gutierrez, J. S., Towery, H., Burks, D. J., Ren, J. M., Previs, S., Zhang, Y., Bernal, D., Pons, S., Shulman, G. I., Bonner-Weir, S., and White, M. F. (1998) Disruption of IRS-2 causes type 2 diabetes in mice. *Nature* **391,** 900–904
42. Jhala, U. S., Canettieri, G., Screaton, R. A., Kulkarni, R. N., Krajewski, S., Reed, J., Walker, J., Lin, X., White, M., and Montminy, M. (2003) cAMP promotes pancreatic β-cell survival via CREB-mediated induction of IRS2. *Genes Dev.* **17,** 1575–1580
43. Park, S., Dong, X., Fisher, T. L., Dunn, S., Omer, A. K., Weir, G., and White, M. F. (2006) Exendin-4 uses Irs2 signaling to mediate pancreatic beta cell growth and function. *J. Biol. Chem.* **281,** 1159–1168
44. Huang, H., Regan, K. M., Wang, F., Wang, D., Smith, D. I., van Deursen, J. M., and Tindall, D. J. (2005) Skp2 inhibits FOXO1 in tumor suppression through ubiquitin-mediated degradation. *Proc. Natl. Acad. Sci. U.S.A.* **102,** 1649–1654
45. Plas, D. R., and Thompson, C. B. (2003) Akt activation promotes degradation of tuberin and FOXO3a via the proteasome. *J. Biol. Chem.* **278,** 12361–12366
46. Xu, C., Kim, N. G., and Gumbiner, B. M. (2009) Regulation of protein stability by GSK3 mediated phosphorylation. *Cell Cycle* **8,** 4032–4039
47. Humphrey, R. K., Yu, S. M., Flores, L. E., and Jhala, U. S. (2010) Glucose regulates steady-state levels of PDX1 via the reciprocal actions of GSK3 and AKT kinases. *J. Biol. Chem.* **285,** 3406–3416
48. Boucher, M. J., Selander, L., Carlsson, L., and Edlund, H. (2006) Phosphorylation marks IPF1/PDX1 protein for degradation by glycogen synthase kinase 3-dependent mechanisms. *J. Biol. Chem.* **281,** 6395–6403
49. Han, S. I., Aramata, S., Yasuda, K., and Kataoka, K. (2007) MafA stability in pancreatic beta cells is regulated by glucose and is dependent on its constitutive phosphorylation at multiple sites by glycogen synthase kinase 3. *Mol. Cell. Biol.* **27,** 6593–6605
50. Guo, S., Burnette, R., Zhao, L., Vanderford, N. L., Poitout, V., Hagman, D. K., Henderson, E., Ozcan, S., Wadzinski, B. E., and Stein, R. (2009) The stability and transactivation potential of the mammalian MafA transcription factor are regulated by serine 65 phosphorylation. *J. Biol. Chem.* **284,** 759–765
51. Maurer, U., Charvet, C., Wagman, A. S., Dejardin, E., and Green, D. R. (2006) Glycogen synthase kinase-3 regulates mitochondrial outer membrane permeabilization and apoptosis by destabilization of MCL-1. *Mol Cell* **21,** 749–760
52. Zhao, Y., Altman, B. J., Coloff, J. L., Herman, C. E., Jacobs, S. R., Wieman, H. L., Wofford, J. A., Dimascio, L. N., Ilkayeva, O., Kelekar, A., Reya, T., and Rathmell, J. C. (2007) Glycogen synthase kinase 3α and 3β mediate a glucose-sensitive antiapoptotic signaling pathway to stabilize Mcl-1. *Mol. Cell. Biol.* **27,** 4328–4339
53. Nihalani, D., Wong, H. N., and Holzman, L. B. (2003) Recruitment of JNK to JIP1 and JNK-dependent JIP1 phosphorylation regulates JNK module dynamics and activation. *J. Biol. Chem.* **278,** 28694–28702
54. Kristiansen, M., Hughes, R., Patel, P., Jacques, T. S., Clark, A. R., and Ham, J. (2010) Mkp1 is a c-Jun target gene that antagonizes JNK-dependent apoptosis in sympathetic neurons. *J. Neurosci.* **30,** 10820–10832
55. Murphy, L. O., Smith, S., Chen, R. H., Fingar, D. C., and Blenis, J. (2002) Molecular interpretation of ERK signal duration by immediate early gene products. *Nat. Cell. Biol.* **4,** 556–564
56. Hoffmann, A., Levchenko, A., Scott, M. L., and Baltimore, D. (2002) The IκB-NF-κB signaling module: temporal control and selective gene activation. *Science* **298,** 1241–1245
57. Kholodenko, B. N. (2006) Cell-signalling dynamics in time and space. *Nat. Rev. Mol. Cell Biol.* **7,** 165–176